

Effective spin model for the spin-liquid phase of the Hubbard model on the triangular lattice

Hong-Yu Yang,¹ Andreas M. Läuchli,² Frédéric Mila,³ and Kai Phillip Schmidt¹

¹*Lehrstuhl für Theoretische Physik I, Otto-Hahn-Straße 4, TU Dortmund, D-44221 Dortmund, Germany*

²*Max Planck Institut für Physik komplexer Systeme, D-01187 Dresden, Germany*

³*Institute of Theoretical Physics, Ecole Polytechnique Fédérale de Lausanne, CH-1004 Lausanne, Switzerland*

We show that the spin liquid phase of the half-filled Hubbard model on the triangular lattice can be described by a pure spin model. This is based on a high-order strong coupling expansion (up to order 12) using perturbative continuous unitary transformations. The resulting spin model is consistent with a transition from three-sublattice long-range magnetic order to an insulating spin liquid phase, and with a jump of the double occupancy at the transition. Exact diagonalizations of both models show that the effective spin model is quantitatively accurate well into the spin liquid phase, and a comparison with the Gutzwiller projected Fermi sea suggests a gapless spectrum and a spinon Fermi surface.

PACS numbers: 75.10.Jm, 75.10.Kt, 05.30.Rt

Although the Hubbard model has been one of the central paradigms in the field of strongly correlated systems for about five decades, new aspects of its extremely rich phase diagram are regularly unveiled. Even at half-filling, the popular wisdom according to which the model has only two phases, a metallic one at weak coupling and an insulating one at strong coupling separated by a first order transition [1], has been recently challenged. This goes back to the work of Morita *et al.* [2] on the triangular lattice which revealed the presence of a non-magnetic insulating phase close to the metal-insulator transition using path integral renormalization group. Further evidence in favour of a phase transition inside the insulating phase has been reported using a variety of theoretical tools [3–6]. More recently, an intermediate spin liquid (SL) phase has also been identified on the honeycomb lattice using Quantum Monte Carlo simulations [7].

The precise nature of the SL phase of the Hubbard model on the triangular lattice is of direct experimental relevance for the 2D organic salt κ -(BEDT-TTF)₂Cu₂(CN)₃ [8]. As such, it has already attracted a lot of attention, but fundamental questions such as the appropriate low-energy effective theory remain unanswered. Since the phase is insulating, an effective model where charge fluctuations are treated as virtual excitations should be possible. One step forward in this direction has been taken by Motrunich [9], who proposed to describe the SL phase with 4-spin interactions. However, whether a description in terms of a pure spin model is possible is far from obvious, in particular since there seems to be a jump in the double occupancy at the transition from the three-sublattice Néel phase to the SL [2, 6].

In this Letter, we show that the correct low-energy theory of both insulating phases, and in particular of the SL phase, is indeed a pure spin model. This has been achieved by deriving an effective spin model to very high order about the strong coupling limit using perturbative continuous unitary transformations (PCUTs), and by showing that it gives a qualitative and quantitative account of the transition from the three-sublattice magnetic order to the SL state. This description gives deep insight into the nature of the SL phase and clearly provides the appropriate framework for further studies.

The starting point is the single-band Hubbard model on the triangular lattice defined by the Hamiltonian

$$\begin{aligned} \mathcal{H} &= H_U + H_t \\ &= U \sum_i n_{i\uparrow} n_{i\downarrow} - t \sum_{\langle i,j \rangle, \sigma} (c_{i\sigma}^\dagger c_{j\sigma} + \text{h.c.}) \end{aligned} \quad (1)$$

where the sum over i runs over the sites of a triangular lattice, and the sum over $\langle i,j \rangle$ over pairs of nearest neighbors. To derive an effective low-energy Hamiltonian, we use PCUTs [10–13] about the localized limit treating the hopping term as a perturbation. The kinetic part can be written as $H_t = t(T_0 + T_1 + T_{-1})$ where T_m changes the number of doubly-occupied sites by m . The PCUT method provides order by order in t/U an effective Hamiltonian H_{eff} with the property $[H_U, H_{\text{eff}}] = 0$, i.e. H_{eff} is block-diagonal in the number of doubly-occupied sites. The low-energy physics at half filling is expected to be contained in the block with no doubly-occupied site H_{eff}^0 , which can be expressed as a spin 1/2 model of the form

$$\begin{aligned} H_{\text{eff}}^0 &= \text{const} + \sum_{\vec{r}, \vec{n}} J_{\vec{n}} (\vec{S}_{\vec{r}} \cdot \vec{S}_{\vec{r}+\vec{n}}) \\ &+ \sum_{\vec{r}, \vec{n}_1, \vec{n}_2, \vec{n}_3} J_{\vec{n}_1, \vec{n}_2}^{\vec{n}_3} (\vec{S}_{\vec{r}} \cdot \vec{S}_{\vec{r}+\vec{n}_1}) (\vec{S}_{\vec{r}+\vec{n}_2} \cdot \vec{S}_{\vec{r}+\vec{n}_3}) + \dots \end{aligned} \quad (2)$$

where \vec{r} and $\vec{r} + \vec{n}_\alpha$ denote sites on the triangular lattice. All remaining terms can be written in a similar way as products of $\vec{S}_{\vec{r}} \cdot \vec{S}_{\vec{r}'}$ due to the SU(2) symmetry of the Hubbard model.

The PCUT provides the magnetic exchange couplings as series expansions in t/U . Since the spectrum of the Hubbard model is symmetric at half filling under the exchange $t \leftrightarrow -t$, only even order contributions are present [14]. We have determined all 2-spin, 4-spin and 6-spin interactions up to order 12. The obtained series are valid in the thermodynamic limit. To this end we have fully exploited for the first time in a PCUT calculation the linked cluster theorem by using graph theory. At order 12 there are 1336 topologically different graphs. The major complication for the determination of higher orders comes from the large number of different

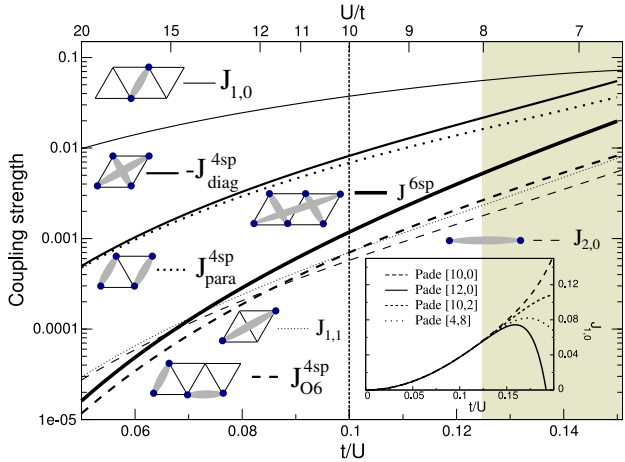


FIG. 1: (Color online) The most relevant exchange couplings displayed as a function of t/U . The 12th order bare series of all couplings appearing up to order 4 and the largest 4-spin interaction J_{O6}^{4sp} plus the largest 6-spin interaction J_{6sp} appearing in order 6 are plotted. Grey shaded area marks the region where extrapolation effects become important. Vertical dashed line indicates the magnetic phase transition. Inset: various Padé approximants as a function of t/U for the nearest-neighbor Heisenberg exchange $J_{1,0}$.

spin operators, which requires to calculate all possible matrix elements for each graph.

The most relevant spin couplings are shown in Fig. 1 as a function of t/U . As already pointed out in Ref. 9, the most important correction to the nearest-neighbor Heisenberg exchange at order 4 are the 4-spin interactions on a diamond plaquette. High-order contributions result in more complex multi-spin interactions with larger spatial extension but also lead to renormalizations of already existing couplings. The latter effect causes for example a sizable splitting of the two 4-spin interactions shown in Fig. 1, which have the same absolute value at order 4. Processes involving sites far apart have small amplitudes, and multi-spin interactions between sites not far from each other are clearly the dominant corrections to the spin operators at order 4.

At large U/t , nearest-neighbour exchange dominates, and the system is expected to develop three-sublattice long-range order [15–17]. Using exact diagonalizations (ED) of clusters up to 36 sites, we have investigated how the properties of the model evolve upon reducing U/t . The most striking feature is a level crossing in the ground state (GS) at $U/t \simeq 10$ (see Fig. 2). This level crossing is observed for all cluster sizes at essentially the same value, which indicates the presence of a first order transition in the thermodynamic limit. Since this ratio is comparable to the critical ratio where other methods have detected a transition into a SL phase, it seems plausible that this level crossing corresponds to this transition. Further investigations below $U/t \simeq 10$ confirm this guess (see below), but let us first investigate to which extent the effective spin model provides an accurate description in this parameter range. The proof that this is so relies on four observations:

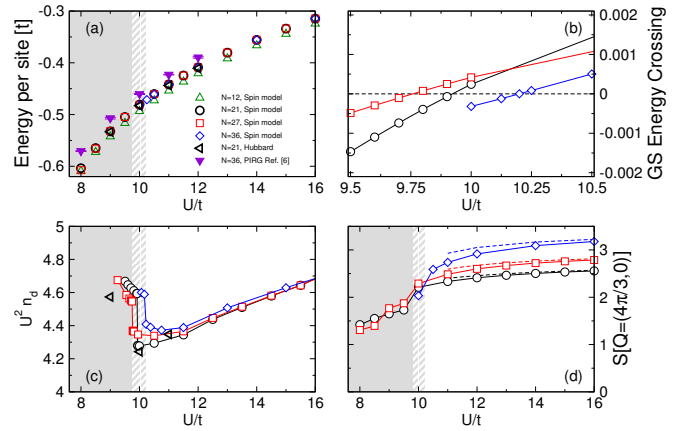


FIG. 2: (Color online) (a) Energy per site as a function of U/t for the Hubbard model and the effective spin model. (b) Level crossings in the effective spin model signalled by the energy difference of the two lowest energies. (c) Double occupancy (times U^2) as a function of U/t . (d) Magnetic structure factor at the 120° AFM ordering wave vector. Dashed lines denotes results for a simplified 2B-4B model evaluated up to order ten. Continuous lines with symbols are the results for the full 2B-4B-6B model considered here. The observable is up to order two in both cases.

- Convergence of the series: As usual, we use Padé approximants to extrapolate the series, and we consider that series are well converged as long as different Padé approximants give consistent results. Here this is definitely true up to $t/U \simeq 0.125$ ($U/t \simeq 8$), i.e. well beyond the level crossing (see inset of Fig. 1). For all couplings, the absolute change between order 10 and 12 is below 10^{-4} (10^{-3}) for $t/U = 0.1$ ($t/U = 0.125$). In fact, clear indications of divergence only appear above $t/U \simeq 0.15$, and this is probably related to the metal-insulator transition.

- Comparison of GS energy with Hubbard model: In view of the anomaly observed at the transition by other approaches [2, 6], it is legitimate to ask whether the GS remains in the sector with no doubly-occupied site. To address this point, we have used ED of finite clusters to calculate the GS energy of both the Hubbard model and the effective spin model as a function of U/t (see Figs. 2a and 2b) up to 21 sites for the Hubbard model, and up to 36 sites for the effective spin model. For the spin model, the total number of spin operators is enormous, and truncating the hierarchy of operators is necessary. We have included in our calculation all spin operators appearing up to order 6. Additionally, we have omitted for a given ratio t/U all terms whose coupling was smaller than 10^{-6} . When embedded on our largest 36 site cluster, this corresponds to $\sim 16'000$ distinct terms in total. The resulting total energies per site are displayed in Fig. 2. The energy per site of the effective spin model depends very little on the size, and for the 21-site cluster, the energies of the Hubbard model and of the effective spin model are in very good agreement on both sides of the transition. This last observation clearly establishes that the effective model remains accurate in the SL

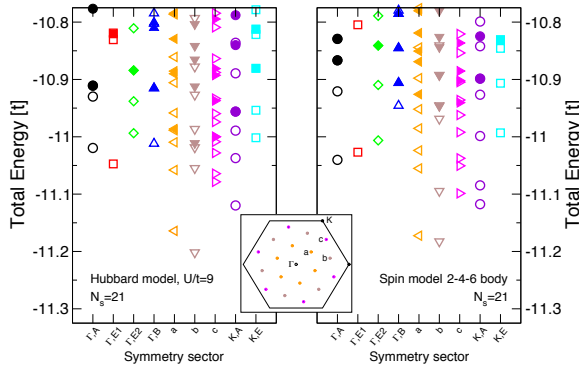


FIG. 3: (Color online) Comparison of the low-energy spectrum of a $N_s = 21$ Hubbard model at $U/t = 9$ (left panel) to results obtained with the effective spin model (right panel). The x -axis labels the different symmetry sectors, while empty (filled) symbols denote $S^z = 1/2$ ($S^z = 3/2$) levels. a, b and c label momenta in the interior of the Brillouin zone.

phase. The GS energies for both the Hubbard model and the effective model are actually significantly lower than recent estimates based on PIRG [6], see Fig. 2a.

- Double occupancy: The comparison of the GS energies suggests that the GS is in the sector of the effective model with no doubly-occupied site in the U/t range considered. This result seems to be incompatible with the jump of the double occupancy n_d reported by other methods for the Hubbard model [2, 6], but in fact it is not because, when calculating the expectation value of observables from the effective model, one must apply the same unitary transformation [12, 18] which, in the present case, leads to a non-zero value of n_d . In practice, it is simpler to use the Feynman-Hellmann theorem which allows to deduce it directly from the energy per site as $n_d = \partial_U \langle \mathcal{H} \rangle / N$. The results are depicted in Fig. 2c. A jump is clearly present at the transition for all finite-size samples as a consequence of the level crossing of the effective model, and its magnitude is consistent with that calculated for the Hubbard model on the 21-site cluster (see Fig. 2c). The significant difference between 21 and 27 sites does not allow to perform a reliable finite-size scaling, but this does not affect the conclusion that the effective spin model captures the double occupancy jump at the transition.

- Low-energy spectrum and GS momentum: It is also important to check how well the effective model reproduces the low-energy spectrum of the original model. To address this issue, we compare the low-energy spectrum at $U/t = 9$ of a $N_s = 21$ Hubbard model with the low-energy excitations of the spin model on the same cluster [25] in Fig. 3. Qualitatively, the agreement is good. In particular, the non-trivial symmetry sectors of the GS and of the first excited states are correctly reproduced. Quantitatively, the difference between the energies (a fraction of a percent) is dominated by the fact that the effective model on a finite cluster should include, starting from order 6, a few processes which wrap around the cluster. These processes are not taken into account in our

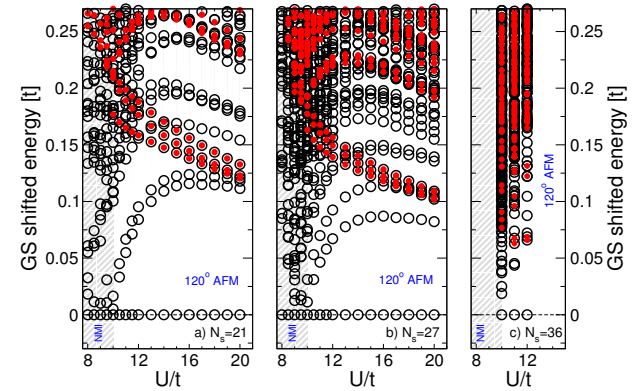


FIG. 4: (Color online) ED spectra of the truncated spin model for (a) $N_s = 21$, (b) $N_s = 27$, and (c) $N_s = 36$ as a function of U/t . Open (black) symbols denote non-magnetic levels. Filled (red) symbols are energy levels corresponding to excitations with finite spin above the GS. The grey shaded area signals the extension of the SL phase.

effective model since they are not present in the thermodynamic limit. The systematic error in the thermodynamic limit is much smaller since it only comes from the precision of the coefficients and the neglect of truncated terms.

The truncated spin model is thus an excellent starting point to investigate the quantum magnetism of the Hubbard model on the triangular lattice. Consequently, we turn to a detailed discussion of its physical properties as a function of U/t . The low-energy ED spectra for clusters of $N_s = 21, 27$, and 36 sites are shown in Fig. 4. For clarity the lowest level at each U/t value is taken as the reference energy and set to zero, and the spatial symmetry quantum numbers of the levels are not specified. For the 36-site cluster, the calculation of the excitation spectrum is numerically very expensive, and it has been performed only for three values of U/t close to the transition, and for a simplified two- and four-spin coupling model (in contrast to the ground state energy calculations in Fig. 2(a) which have been performed based on the more demanding model with the aforementioned cutoff 10^{-6}). At large U/t (down to $U/t \sim 15$), the level structure revealed by the 21 and 27-site clusters is typical of the tower of states of a 120° antiferromagnet (AFM) [15]. For smaller U/t ratios, some levels start to bend down and to deviate from the leading $1/U$ behavior of the Heisenberg regime. Drastic changes occur in the spectrum at $U/t \approx 10$. First of all, on *all* clusters, excited states with different quantum numbers cross the large U/t GS level. Besides, a large number of singlets accumulate at low energy in both the effective spin model *and* the Hubbard model for $U/t \leq 10$.

To better characterize this change of behaviour, we have calculated the structure factor corresponding to the three-sublattice 120° order as a function of t/U by implementing the unitary transformation on the observable at order t^2/U^2 . Above the level crossing, this structure factor increases with the size, as expected for a long-range ordered phase. By contrast, below the level crossing - i.e. in the putative SL region

- the structure factor is finite size saturated, implying either short range correlations, or an algebraic decay with a sizeable decay exponent. At large U/t , the slight reduction of the structure factor is mainly a consequence of the admixture of empty and doubly occupied sites, which reduces the effective local spin length S^2 below 3/4. However, as we approach the level crossing, the extra terms in the spin Hamiltonian further reduce the structure factor, as can be seen by comparing the results for the 'full' effective model with those for a truncated model where only the 2-spin and 4-spin terms that appear at fourth order (but evaluated using the full series) are kept (see Fig. 2d). So one cannot exclude that the long-range magnetic order disappears slightly before the level crossing.

The issue of the spin gap in the SL phase requires a careful discussion. Indeed, the energy of the first magnetic excitation is nearly constant between 21 and 27 sites and drops dramatically for 36 sites. So depending upon whether one includes the 36 cluster or not, finite-size effects suggest a vanishing gap or a finite gap. Now, the significant difference between the 36-site cluster and the other two might be due to an even-odd N_s effect, or to the use of a simplified model, and it might be better not to include it in the finite-size analysis. Now, concentrating on the 21 and 27 site clusters, the energy of the first magnetic excitation is indeed almost constant, but if one looks carefully at the drastic U/t dependence of the excited magnetic levels when approaching the SL regime from large U/t , some excitations bend down, and their energy decreases very significantly between 21 and 27 sites, possibly leading to a gap closing in the thermodynamic limit. So it is difficult to decide on the presence of a spin gap based on the available ED data alone. In the next paragraph we show that the data can be interpreted from a broader perspective.

In his seminal paper Motrunich [9] proposed a plain Gutzwiller projected Fermi sea as a prototype spin wave function for the SL phase on the triangular lattice. This idea later materialized into a theory of Spin Bose Metal (SBM) phases [20] (see Ref. [21] for a related scenario), which has been successfully applied to a one-dimensional triangular strip model with two- and four-spin interactions [20, 22]. Interestingly, the numerical low-energy spectrum of the triangular strip in the SBM phase looks qualitatively similar to the spectrum we observe on the triangular lattice, with respect to both the dense excitation spectrum with many low energy singlets and the irregular finite size behavior of the spin gap [22]. A second remarkable agreement between the SBM picture by Motrunich and our ED analysis comes from the quantum numbers of the ground state wave function in the SL region. On the $N_s = 27$ site sample for example the noninteracting half filled Fermi sea has a sixfold degenerate ground state momentum. This prediction matches precisely the ground state quantum number of the effective spin model in the SL region adjacent to the magnetically ordered phase. On the other samples ($N_s = 21, 36$) the Fermi sea ground state degeneracy is larger and thus less constraining, but the ground state quantum numbers of the SL regime are still compatible with this picture.

In conclusion, we have derived the appropriate low-energy

theory of the non-magnetic phase of the half-filled Hubbard model on the triangular lattice. It is a pure spin model with multi-spin exchange. Furthermore, we have performed an ED investigation of this model. Several aspects of the results are compatible with the SBM picture predicting a gapless spectrum with a spinon Fermi surface. It will be interesting to extend our investigation to the anisotropic triangular lattice [23, 24], and to compare the results directly to the SL material κ -(BEDT-TTF)₂Cu₂(CN)₃ and to the other members of the family. Finally, this approach is also applicable to other, possibly frustrated lattice topologies for which similarly interesting Mott phases can be expected.

We thank R. McKenzie for fruitful discussions and T. Yoshioka for providing PIRG data for comparison. K.P.S. acknowledges ESF and EuroHorcs for funding through his EURYI. The ED have been enabled through computing time allocated at ZIH TU Dresden and the MPG RZ Garching. F.M. acknowledges the financial support of the Swiss National Fund and of MaNEP.

-
- [1] A. Georges *et al.*, Rev. Mod. Phys. **68**, 041101 (1996).
 - [2] H. Morita, S. Watanabe, and M. Imada, J. Phys. Soc. Jpn. **71**, 2109 (2002).
 - [3] B. Kyung and A.M.S. Tremblay, Phys. Rev. Lett. **97**, 046402 (2006).
 - [4] P. Sahebsara and D. Sénéchal, Phys. Rev. Lett. **100**, 136402 (2008).
 - [5] L.F. Tocchio *et al.*, Phys. Rev. B. **78**, 041101 (2008).
 - [6] T. Yoshioka, A. Koga, and N. Kawakami, Phys. Rev. Lett. **103**, 036401 (2009).
 - [7] Z.Y. Meng *et al.*, Nature **464**, 847 (2010).
 - [8] Y.S. Shimizu *et al.*, Phys. Rev. Lett. **91**, 107001 (2003).
 - [9] O. L. Motrunich, Phys. Rev. B **72**, 045105 (2005).
 - [10] J. Stein, J. Stat. Phys. **88**, 487 (1997).
 - [11] C. Kneller and G. S. Uhrig, Eur. Phys. J. B **13**, 209 (2000).
 - [12] C. Kneller, K. P. Schmidt, and G. S. Uhrig, J. Phys. A **36**, 7889 (2003).
 - [13] A. Reischl, E. Müller-Hartmann, and G.S. Uhrig, Phys. Rev. B **70**, 245124 (2004).
 - [14] A. H. MacDonald, S. M. Girvin, and D. Yoshioka, Phys. Rev. B **37**, 9753 (1988).
 - [15] B. Bernu, C. Lhuillier, and L. Pierre, Phys. Rev. Lett. **69**, 2590 (1992).
 - [16] L. Capriotti, A. E. Trumper, and S. Sorella, Phys. Rev. Lett. **82**, 3899 (1999).
 - [17] S. R. White and A. L. Chernyshev, Phys. Rev. Lett. **99**, 127004 (2007).
 - [18] J.-Y. P. Delannoy *et al.*, Phys. Rev. B **72**, 115114 (2005).
 - [19] W. LiMing *et al.*, Phys. Rev. B **62**, 6272 (2000).
 - [20] D.N. Sheng, O.I. Motrunich, and M.P.A. Fisher, Phys. Rev. B **79**, 205112 (2009).
 - [21] S.-S. Lee and P.A. Lee, Phys. Rev. Lett. **95**, 036403 (2005).
 - [22] A. D. Kliorinomos *et al.*, Phys. Rev. B **76**, 075302 (2007).
 - [23] H.C. Kandal *et al.*, Phys. Rev. Lett. **103**, 067004 (2009).
 - [24] K. Nakamura *et al.*, J. Phys. Soc. Jap. **78**, 083710 (2009).
 - [25] The largest Hilbert space sector of the Hubbard model (spin model) has dim $\sim 6 \times 10^9$ (dim $\sim 10^5$).